Annealing temperature effects on ferromagnetism and structure of Si1−xMnx films prepared by magnetron sputtering

ARTICLE *in* VACUUM · MARCH 2012

Impact Factor: 1.86 · DOI: 10.1016/j.vacuum.2012.01.001

Guoliang Peng
Wuhan University

Bo He
University of Science and Technology of Ch…

Zhiyun Pan
University of Science and Technology of Ch…

Zhongpo Zhou
Wuhan University

Vacuum 86 (2012) 1358–1362

Contents lists available at SciVerse ScienceDirect

Vacuum

journal homepage: www.elsevier.com/locate/vacuum

Annealing temperature effects on ferromagnetism and structure of $Si_{1-x}Mn_x$ films prepared by magnetron sputtering

Tiecheng Li [a], Liping Guo [a,*], Congxiao Liu [b], Guoliang Peng [a], Bo He [c], Zhiyun Pan [c], Zhongpo Zhou [a], Shuigang Xu [a], Zuci Quan [a]

[a] Key Laboratory of Artificial Micro- and Nano-structures of Ministry of Education and School of Physics and Technology, Wuhan University, Wuhan 430072, China
[b] Department of Physics, Chemistry, and Mathematics, Alabama A&M University, 4900 Meridian Street, Normal, AL 35762, USA
[c] National Synchrotron Radiation Laboratory, University of Science & Technology of China, Hefei 230029, China

ARTICLE INFO

Article history:
Received 6 May 2011
Received in revised form
24 December 2011
Accepted 1 January 2012

Keywords:
Magnetron sputtering
Diluted magnetic semiconductors
X-ray absorption near-edge structure
Post-rapid thermal annealing

ABSTRACT

$Si_{1-x}Mn_x$ diluted magnetic semiconductor films were deposited on the p-Si (100) single crystal wafer using magnetron sputtering method. Post-rapid thermal annealing treatments were performed at temperatures of 700 °C, 800 °C, and 900 °C in an argon atmosphere for approximately 5 min. Alternating gradient magnetometer, scanning electron microscope, atomic force microscope, X-ray diffraction and X-ray absorption near-edge structure spectra were employed to characterize magnetic properties and structure of the as-grown and annealed films. The films were about 2.8 μm thick and the RMS roughness of the surface was about 5–10 nm. All samples exhibit ferromagnetism at room temperature and the saturation magnetization reaches at the maximum value for the sample annealed at 700 °C. The silicide $MnSi_{1.7}$ was observed in the annealed samples. X-ray absorption near-edge structure spectra indicated that Mn atoms preferred to occupy substitutional or interstitial sites instead of precipitating to form silicide when annealing at 700 °C. It is inferred that the observed ferromagnetism is attributed to the interstitial and substitutional Mn dimers, which existed mostly in the sample annealed at 700 °C. The weaker ferromagnetism of the 900 °C annealed sample was closely related to the increased content of Mn_4Si_7 compound.

1. Introduction

Diluted magnetic semiconductors (DMSs) have attracted much attention because of their potential application in electronic devices that utilize both charge and spin of electrons [1–8]. It is highly desired that ferromagnetic semiconductors be fabricated with most widely used conventional elemental semiconductors by appropriate doping with transition metal ions such as Mn. Spintronic devices based on conventional elemental semiconductors are believed to be significant due to the matured processing technology in modern electronics and compatibility between the spintronics devices and the active electronic devices. Most of these investigations involving DMSs have been focused on Mn-doped III–V [9] or II–VI [10] group materials. On the other hand, despite the technological importance of Si-compatible materials, less effort has been directed toward the synthesis of transition-metal-doped Si [11–15].

Because the equilibrium solubility of transition metals in Si is extremely low, nonequilibrium techniques have been used to induce Mn atoms into the silicon crystal lattice [16–18]. Silicon heavily doped with Mn at the doping levels more than 5% have been grown by using magnetron sputtering [19–21], with a curie temperature above 250 K. It was found that the ferromagnetism was affected by concentration of Mn atoms, thermal annealing conditions, and carriers of the Si substrate. Although it is recognized that the doping Mn atoms play a key role in ferromagnetism, the location of Mn in Si substrate and local surroundings around Mn atoms in $Si_{1-x}Mn_x$ DMSs films still keep unresolved.

X-ray absorption near-edge spectroscopy (XANES) is a unique technique for probing the locations of magnetic ions in the semiconductor. This technique has been widely used to identify the role of Mn in magnetism of III–V and II–VI group DMSs, and recently was used by Wolska et al. to investigate local structure around Mn in Mn implanted Si [22,23].

In the present paper, DMS $Si_{1-x}Mn_x$ films were deposited by magnetron sputtering and annealed at 700 °C, 800 °C, and 900 °C. By analyzing the results of XANES together with scanning electron microscope (SEM), atomic force microscope (AFM), and X-ray

* Corresponding author. School of Physics and Technology, Wuhan University, Wuhan 430072, China. Tel.: +86 27 6875 2481x2223; fax: +86 27 6875 2569.
E-mail addresses: guolp@whu.edu.cn, guolp99@sohu.com (L. Guo).

0042-207X/$ – see front matter © 2012 Elsevier Ltd. All rights reserved.
doi:10.1016/j.vacuum.2012.01.001

diffraction (XRD), microstructure of the as-grown and annealed samples was investigated and the possible origin of magnetism in the $Si_{1-x}Mn_x$ films was discussed.

2. Experiments

$Si_{1-x}Mn_x$ thin films were deposited on p-typed Si (100) wafer at room temperature by radio frequency (RF) magnetron sputtering method. Prior to the deposition, the silicon substrates were ultrasonically cleaned in acetone and alcohol in sequence. The thin films were sputtered from a Mn/Si composite target, in which small Mn pellets were uniformly distributed on single crystalline Si (100) disk with a Si/Mn area ratio of 19:1. The purity of Mn pellets was 99.9%. During the deposition, the Ar pressure and the RF sputtering power were controlled at 1 Pa and 10 W, respectively. The sputter time was 10 h, and the average deposition rate was slightly less than 300 nm/h.

In order to understand the effect of annealing on $Si_{1-x}Mn_x$ films, rapid thermal annealing (RTA) was carried out after deposition. The films were annealed in an argon atmosphere at temperature of 700 °C, 800 °C, and 900 °C for 5 min.

Cross-section micrograph was observed using a SEM (FEI SironMP SEM system) and the composition of $Si_{1-x}Mn_x$ films was determined by using an energy dispersive spectroscopy (EDS) system (EDAX genesis 7000) operated at 12 kV. Surface morphology was analyzed using an AFM (Shimadzu SPM-9500J3) operated in contact mode. Magnetic hysteresis loops were measured at room temperature using a high-sensitivity (10^{-11} $A \cdot m^2$ sensitivity) alternating gradient magnetometer (PMC 2900-04C). Structure of the deposited $Si_{1-x}Mn_x$ films was characterized by XRD (Bruker-axs D8 advanced) with a Cu Kα radiation.

XANES spectra were measured for all investigated samples at the U7C station, National Synchrotron Radiation Laboratory (NSRL), Hefei, China. The double-crystal Si (111) monochromators at the U7C station ensures a resolution of $dE/E = 3 \times 10^{-4}$. The storage ring was operated at 800 MeV with a typical current of 100∼300 mA. Measurement was carried out at the Mn K edge using the X-ray fluorescence detection method.

3. Results and discussion

The relative content of manganese in the as-grown $Si_{1-x}Mn_x$ film is 8% ($x = 0.08$), determined by EDS system (Fig. 1). Annealing as-grown samples could result in the diffusion of Si from the substrate into $Si_{1-x}Mn_x$ film. However, since we used the single crystalline Si (100) wafer as the substrate, only minute quantity of Si was expected to diffuse from the substrate into films upon annealing, which would give little contribution to the change of Mn concentration. Consequently, we consider that all the annealed samples are showing the same Si/Mn composition with the as-grown sample. The cross-section SEM micrograph of the as-grown $Si_{1-x}Mn_x$ sample is shown in Fig. 2. The image indicates that the film is about 2.84 μm thick. Fig. 3 shows the surface morphology, for which small difference is present for different samples. Some big island-like humps can be recognized in the samples annealed at 700 °C and 900 °C.

For the as-grown and all annealed samples, room-temperature ferromagnetism was observed with magnetic hysteresis (Fig. 4). The value of mean square roughness (RMS) and the saturation magnetization (Ms) of the samples are given in Table 1. The results indicate that the sample annealed at 700 °C has the maximum RMS and Ms values. Given the similarity of the AFM images of the as-grown sample and the sample annealed at 800 °C, we suspect that the difference of the surface morphology for the samples is due to the variation of sputtering condition in the preparation process, rather than an effect of annealing.

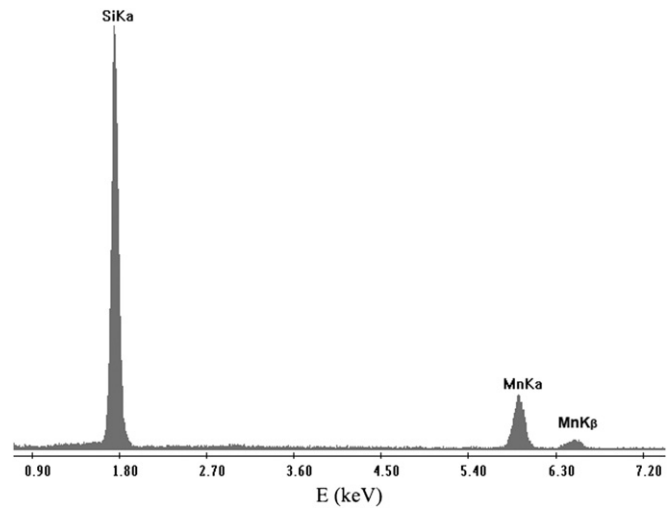

Fig. 1. EDS spectrum of the as-grown $Si_{1-x}Mn_x$ sample.

Fig. 5 shows θ-2θ scan of samples by Lab-XRD. The spectra have been normalized according to the intensity and position of Si (200) peak. They clearly indicate that the annealed films were crystallized, while the unannealed sample was amorphous. A set of weak peaks marked in the figure were originated from higher manganese silicides with Si composition of around 1.7 [24], such as Mn_4Si_7, which exhibits weak ferromagnetism at 47 K [25]. These rich varieties of Mn silicides are extremely difficult to identify [26]. For that reason, all different compositions are named as $MnSi_{1.7}$ here. The amorphous $MnSi_{1.7}$ phase was found in the as-grown sample. No other mixed phase existed in the annealed films except the silicon and a small amount of $MnSi_{1.7}$ phase. The content and the exact compositions of $MnSi_{1.7}$ phase change with the increase of annealing temperature. This is confirmed by the observation that as annealing temperature increased from 700 °C to 800 °C, there is a shift in diffraction peak and peak intensity changes in XRD spectrum. Liu et al. [20] suggested that it is possible for manganese atoms to incorporate into the silicon lattice, which could be verified by XANES.

The FEFF 8.2 code [27] enabling theoretical calculation of the XANES spectra for different models was used to determine possible surrounding environments of Mn atoms. The measured

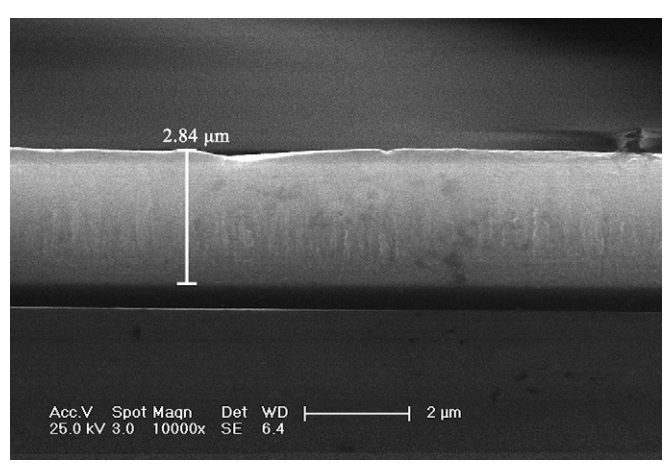

Fig. 2. Cross-section SEM image of the as-grown $Si_{1-x}Mn_x$ sample.

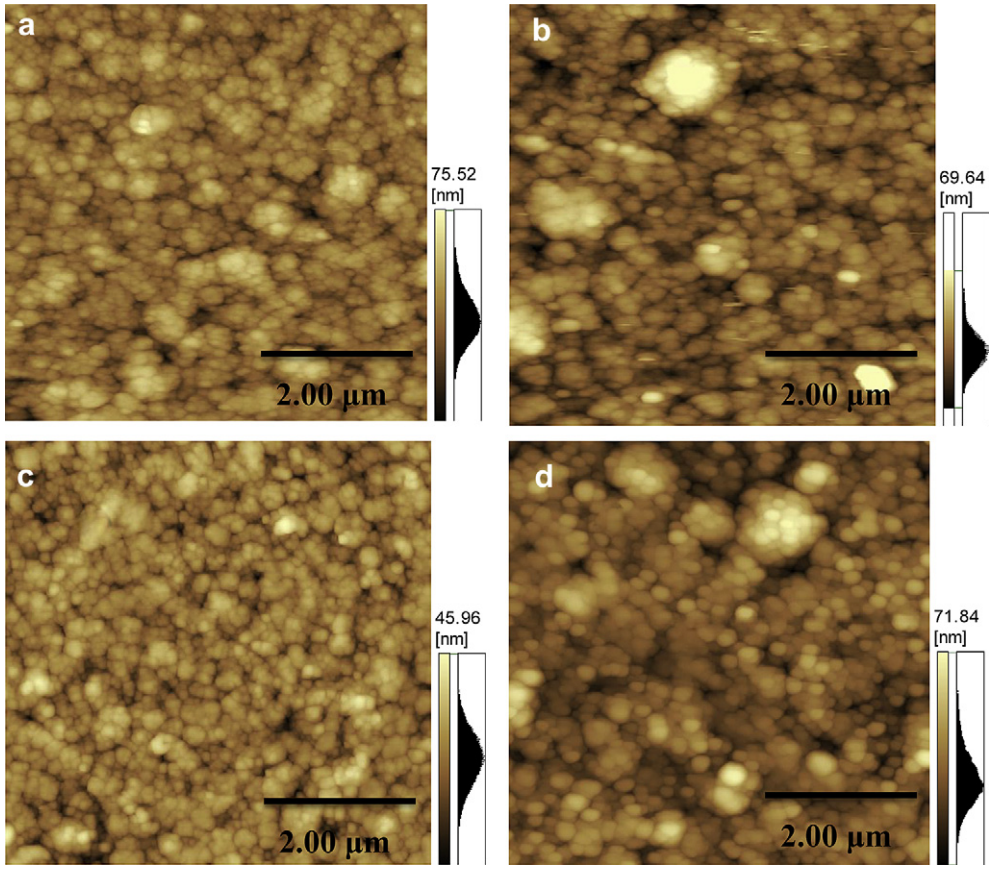

Fig. 3. AFM images of (a) the as-grown sample, the samples annealed at (b) 700 °C, (c) 800 °C, and (d) 900 °C.

XANES spectrum of standard Mn foil and the calculated XANES spectra of Mn_{int} (Mn atoms in interstitial position, including the tetrahedral position $Mn_{t\text{-}int}$ and the hexagonal position $Mn_{h\text{-}int}$), Mn_{sub} (Mn atoms in substitutional position), and Mn_4Si_7 models are shown in Fig. 6. The illustrations of Mn_4Si_7, $Mn_{h\text{-}int}$, $Mn_{t\text{-}int}$, and Mn_{sub} models are shown in Fig. 7. In the calculated models, a perfect silicon matrix was used as a basis for the Mn_{int} and Mn_{sub} cases. About 8 percent doped Mn atoms were placed in a silicon cluster with 148 silicon atoms (i.e., 10 shells). The Hedin–Lundqvist exchange correlation potential, the self-consistence-field (SCF), XANES, and full multiple scattering (FMS) cards were applied in all cases.

As shown in Fig. 6, the spectrum of standard Mn differs significantly from that of $Si_{1-x}Mn_x$ samples. The $Mn_{h\text{-}int}$ spectrum also does not resemble the observed shape of the experimental spectrum. Therefore, the assumption that Mn atoms formed Mn clusters or $Mn_{h\text{-}int}$ structure can be ruled out. The shoulder peak A in the samples was devoted to the Mn_4Si_7 compound, which indicated that silicide Mn_4Si_7 existed in the annealed samples. Peak B in the 700 °C annealed sample was attributed to the $Mn_{t\text{-}int}$ model. As the annealing temperature increases, peak B is shifted toward higher energy, close to the peak of Mn_4Si_7, suggesting that more Mn_4Si_7 formed in the samples annealed at 800 °C and 900 °C. Peak C for the samples annealed at 700 °C and 800 °C was attributed to the Mn_{sub} model, implying that annealing promoted the motion of Mn atoms to the substitutional position. On the other hand, in the sample annealed at 900 °C, more $MnSi_{1.7}$ phase was precipitated from the silicon lattice. This led to a decrease of the $Mn_{t\text{-}int}$ and Mn_{sub} atoms, evidenced both by XANES spectrum and XRD patterns. As for the as-grown sample, the XANES spectrum indicates that there exist clusters with short-range order structure close to Mn_4Si_7 and Mn_{sub}. This is consistent with the XANES spectrum and XRD patterns where broad diffraction hump of Mn_4Si_7 was observed for this sample (Fig. 5), showing amorphous structure for the sample. In summary, the XANES results suggest that Mn_{sub} and Mn_{int} atoms existed mostly in the 700 °C annealed sample.

It has been found, by the model calculation, that the pairs of Mn spins coupled to the matrix valence band states have a lower

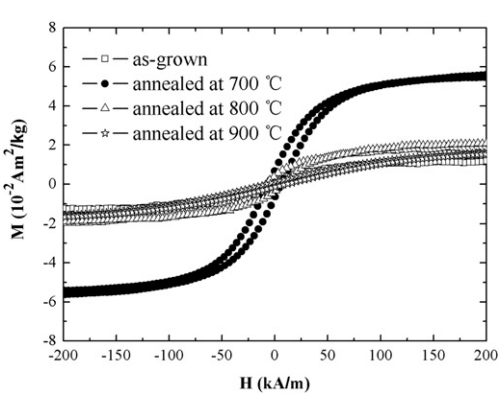

Fig. 4. Magnetic hysteresis loops of the as-grown and annealed samples measured at room temperature.

Table 1
RMS roughness and Ms values of the as-grown and annealed samples.

Sample	As-grown	Annealed at 700 °C	Annealed at 800 °C	Annealed at 900 °C
RMS (nm)	8.722	10.855	5.686	9.645
Ms (Am^2/kg)	1.3×10^{-2}	5.5×10^{-2}	1.9×10^{-2}	1.6×10^{-2}

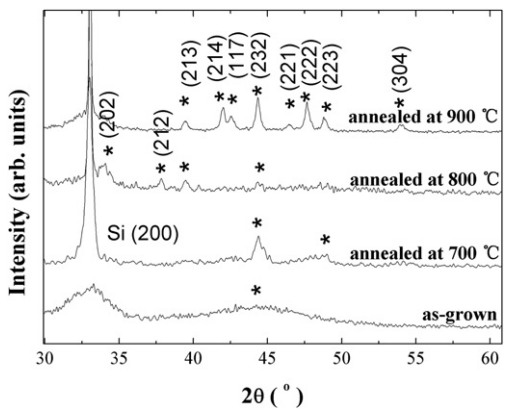

Fig. 5. Comparison of XRD spectra for the as-grown and annealed samples.

energy in the ferromagnetic configuration than they would have in the antiferromagnetic one [28]. The formation energy of Mn and Mn dimers is lower than the sum of the separate constituents, and in p-typed Si the most stable configuration involving up to two Mn atoms is the Mn_{sub}-Mn_{int} complex, which shows a ferromagnetism spin alignment that allows a net magnetization of material [29].

The above theoretical prediction is in good agreement with our experimental results. As indicated by the XANES spectrum, with less content of $MnSi_{1.7}$ precipitated in the sample annealed at 700 °C, Mn_{sub} and $Mn_{t\text{-}int}$ atoms largely coexisted. The Mn_{sub}-Mn_{int} dimer was relatively dominating and the sample showed strongest ferromagnetism among all samples. On the other hand, the increased content of Mn_4Si_7 in other annealed samples could be a factor weakening the ferromagnetism. With the increase of annealing temperature, the content of Mn_4Si_7 phase increased and the numbers of Mn_{sub} and $Mn_{t\text{-}int}$ atoms decreased, preventing the formation of Mn_{sub}-Mn_{int} dimers with a ferromagnetism spin alignment.

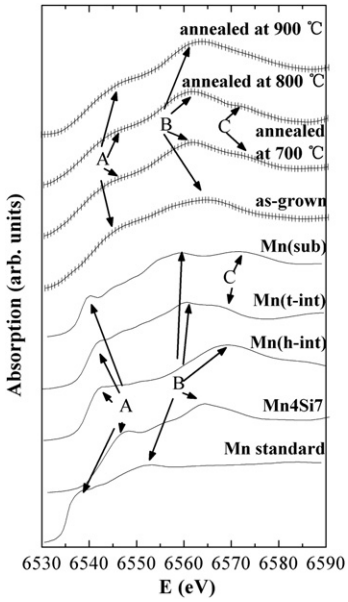

Fig. 6. Comparison of XANES spectra for the as-grown and annealed samples, as well as calculated models: Mn standard (metal Mn), Mn_4Si_7, $Mn_{t\text{-}int}$ model (Mn atoms in tetrahedral interstitial position), $Mn_{h\text{-}int}$ model (Mn atoms in the hexagonal position), and Mn_{sub} model (Mn atoms in substitutional position).

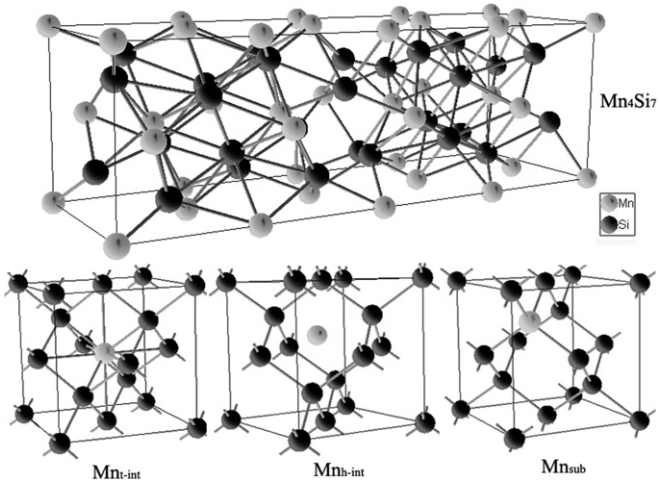

Fig. 7. Illustrations of Mn_4Si_7, $Mn_{h\text{-}int}$, $Mn_{t\text{-}int}$, and Mn_{sub} models.

4. Summary

In summary, $Si_{1-x}Mn_x$ films deposited by magnetron sputtering and post-annealing exhibited ferromagnetism property at room temperature. After annealing, the $Si_{1-x}Mn_x$ films crystallized and $MnSi_{1.7}$ precipitated in the samples. Among the as-grown and annealed samples, largest value of saturation magnetization was found in the sample annealed at 700 °C. Mn_{sub} and $Mn_{t\text{-}int}$ atoms were detected by XANES to coexist mostly in this sample. This evidence supported the theoretical prediction that the ferromagnetism in $Si_{1-x}Mn_x$ system originated from the ferromagnetic interaction between the interstitial and substitutional Mn atoms. Weaker ferromagnetism in the samples annealed at 900 °C was closely related to the increased content of Mn_4Si_7 compound.

Acknowledgment

The work was supported by National Natural Science Foundation of China under Grant No. 11075119 and 10775108, National Science Fund for Talent Training in Basic Science under Grant No. J0830310, and the Fundamental Research Funds for the Central Universities under Grant No. 20102020201000034.

References

[1] Prinz GA. Science 1998;282:1660–3.
[2] Park JH, Vescovo E, Kim HJ, Kwon C, Ramesh R, Venkatesan T. Nature 1998; 392:794–6.
[3] Wolf SA, Awschalom DD, Buhrman RA, Daughton JM, Von Molnar S, Roukes ML, et al. Science 2001;294:1488–95.
[4] Zhu HJ, Ramsteiner M, Kostial H, Wassermeier M, Schonherr HP, Ploog KH. Phys Rev Lett 2001;87:016601.
[5] Ball P. Nature 2000;404:918–20.
[6] Pearton SJ, Abernathy CR, Norton DP, Hebard AF, Park YD, Boatner LA, et al. Mater Sci Eng R 2003;40:137–68.
[7] Macdonald AH, Schiffer P, Samarth N. Nat Mater 2005;4:195–202.
[8] Zhou SQ, Potzger K, Xu QY, Talut G, Lorenz M, Skorupa W, et al. Vaccum 2009; 83:513–9.
[9] Ohno H. Science 1998;281:951–6.
[10] Mukherjee D, Dhakal T, Srikanth H, Mukherjee P, Witanachchi S. Phys Rev B 2010;81:205202.
[11] Nakayama H, Ohtab H, Kulatovc E. Physica B 2001;302/303:419–24.
[12] Kim HM, Kim NM, Park CS, Yuldashev SU, Kang TW, Chung KS. Chem Mater 2003;15:3964–5.
[13] Zhang YT, Jiang Q, Smith DJ, Drucker J. J Appl Phys 2005;98:033512.
[14] Lin HT, Huang WJ, Wang SH, Lin HH, Chin TS. J Phys Condens Matter 2008;20: 095004.
[15] Demidov ES, Aronzon BA, Gusev SN, Karzanov VV, Lagutin AS, Lwsnikov VP, et al. J Magn Magn Mater 2009;321:690–4.

[16] Yoon IT, Park CJ, Kang TW. J Magn Magn Mater 2007;311:693–6.
[17] Jung W, Misiuk A. Vacuum 2007;81:1408–10.
[18] Peng NH, Jeynes C, Bailey MJ, Adikaari D, Stolojan V, Webb RP. Nucl Instrum Meth B 2009;267:1623–5.
[19] Zhang FM, Liu XC, Gao J, Wu XS, Du YW, Zhu H, et al. Appl Phys Lett 2004;85:786–8.
[20] Liu XC, Lu ZH, Lu ZL, Lv LY, Wu XS, Zhang FM, et al. J Appl Phys 2006;100:073903.
[21] Liu XC, Lin YB, Wang JF, Lu ZH, Lu ZL, Xu JP, et al. J Appl Phys 2007;102:033902.
[22] Wolska A, Lawniczak-Jablonska K, Klepka M, Walczak MS, Misiuk A. Phys Rev B 2007;75:113201.
[23] Soo YL, Yao JH, Wang CS, Chang SL, Hsieh CA, Lee JF, et al. Phys Rev B 2010;81:104104.
[24] Zhou SQ, Potzger K, Zhang GF, Mücklich A, Eichhorn F, Schell N, et al. Phys Rev B 2007;75:085203.
[25] Gottlieb U, Sulpice A, Lambert-Andron B, Laborde O. J Alloys Compd 2003;361:13–8.
[26] Eizenberg M, Tu KN. J Appl Phys 1982;53:6885.
[27] Ankudinov AL, Ravel B, Rehr JJ, Conradson SD. Phys Rev B 1998;58:7565–76.
[28] Inoue J, Nonoyama S, Itoh H. Phys Rev Lett 2000;85:4610–3.
[29] Bernardinia F, Picozzi S, Continenza A. Appl Phys Lett 2004;84:2289–91.